

ANISOTROPIC LATTICE QCD STUDIES OF PENTA-QUARK ANTI-DECUPLET *

N. ISHII¹, T. DOI², H. IIDA¹, M. OKA¹, F. OKIHARU³, H. SUGANUMA¹

¹ *Dept. of Phys., Tokyo Institute of Technology, Meguro, Tokyo 152-8551, Japan*

² *RIKEN BNL Research Center, BNL, Upton, New York 11973, USA*

³ *Faculty of Science and Tech., Nihon Univ., Chiyoda, Tokyo 101-8308, Japan*

Anti-decuplet penta-quark baryon is studied with the quenched anisotropic lattice QCD for accurate measurement of the correlator. Both the positive and negative parity states are studied using a non-NK type interpolating field with $I = 0$ and $J = 1/2$. After the chiral extrapolation, the lowest positive parity state is found at $m_{\Theta} \simeq 2.25$ GeV, which is too massive to be identified with the experimentally observed $\Theta^+(1540)$. The lowest negative parity state is found at $m_{\Theta} \simeq 1.75$ GeV, which is rather close to the empirical value. To confirm that this state is a compact 5Q resonance, a new method with “*hybrid boundary condition (HBC)*” is proposed. The HBC analysis shows that the observed state in the negative parity channel is an NK scattering state.

1. Introduction

LEPS group at SPring-8 has discovered a narrow resonance $\Theta^+(1540)$, which is centered at 1.54 ± 0.01 GeV with a width smaller than 25 MeV.¹ This resonance is confirmed to have baryon number $B = 1$, charge $Q = +1$ and strangeness $S = +1$ implying that it is a baryon containing at least one \bar{s} . Hence, its simplest configuration is $uudd\bar{s}$, i.e., a manifestly exotic penta-quark (5Q) state. The experimental discovery of Θ^+ was motivated by a theoretical prediction.²

Tremendous theoretical efforts have been and are still being devoted to the investigation of Θ^+ ,^{3,4} among which its parity is one of the most important topics. Experimentally, the parity determination of Θ^+ is quite challenging,^{5,6} while opinions are divided in the theoretical side.³

There are several quenched lattice QCD studies of the 5Q state,^{7,8,9,10} However, the results have not yet reached a consensus. One group⁹ claims the existence of a low-lying positive parity 5Q resonance. Negative parity 5Q resonance is claimed by two groups,^{7,8} among which Ref. 8 has omitted a quark-exchange diagram between diquark pairs assuming the highly

*Lattice QCD numerical calculation has been done with NEC SX-5 at Osaka University.

correlated diquark picture. Note that these three groups employed non-NK type interpolating fields. In contrast, Ref. 10 has employed the NK-type interpolating field, and performed solid analysis concluding that no signal for a 5Q resonance state is observed. There is another type of lattice QCD studies of the static 5Q potential¹¹ aiming at providing physical insights into the structure of 5Q baryons.

In this paper, we study the 5Q baryon Θ^+ for both parities by using high-precision data generated with the quenched anisotropic lattice QCD. We employ the standard Wilson gauge action at $\beta = 5.75$ on the $12^3 \times 96$ lattice with the renormalized anisotropy $a_s/a_t = 4$. The anisotropic lattice method is a powerful technique, which can provide us with high-precision data quite efficiently.^{12,13,14,15} The lattice spacing is determined from the static quark potential adopting the Sommer parameter $r_0^{-1} = 395$ MeV leading to $a_s^{-1} = 1.100(6)$ GeV ($a_s \simeq 0.18$ fm).¹³ The lattice size $12^3 \times 96$ amounts to $(2.15\text{fm})^3 \times 4.30\text{fm}$ in the physical unit. The $O(a)$ -improved Wilson quark (clover) action is employed¹³ with four values of hopping parameters as $\kappa = 0.1210(0.0010)0.1240$, which roughly covers $m_s \leq m_q \leq 2m_s$ corresponding to $m_\pi/m_\rho = 0.81, 0.77, 0.72$ and 0.65 . By keeping $\kappa_s = 0.1240$ fixed for s quark, we change $\kappa = 0.1210 - 0.1240$ for u and d quarks for chiral extrapolation. Unless otherwise indicated, we use

$$(\kappa_s, \kappa) = (0.1240, 0.1220), \quad (1)$$

as a typical set of hopping parameters. Anti-periodic boundary condition (BC) is imposed on the quark fields along the temporal direction. To enhance the low-lying spectra, we adopt a smeared source with the gaussian size $\rho \simeq 0.4$ fm. We use 504 gauge configurations to construct correlators of Θ^+ . For detail, see Ref. 16.

In the former part of this paper, we present the standard analysis of 5Q correlators in both the positive and the negative parity channels adopting the standard periodic boundary condition along spatial directions. Latter half of this paper is devoted to a further investigation of the negative parity state. Proposing a new general method with “*hybrid boundary condition (HBC)*”, we attempt to determine whether it is a compact resonance state or a NK scattering state.

2. Parity projection

We consider a non-NK type interpolating field for Θ^+ as

$$O \equiv \epsilon_{abc}\epsilon_{ade}\epsilon_{bfg} (u_d^T C \gamma_5 d_e) (u_f^T C d_g) (C \bar{s}_c^T), \quad (2)$$

where $a - g$ denote color indices, and $C \equiv \gamma_4 \gamma_2$ denotes the charge conjugation matrix. The quantum number of O is spin $J = 1/2$ and isospin $I = 0$. Under the spatial reflection of the quark fields, i.e., $q(t, \vec{x}) \rightarrow \gamma_4 q(t, -\vec{x})$, O transforms exactly in the same way, i.e., $O(t, \vec{x}) \rightarrow +\gamma_4 O(t, -\vec{x})$, which means that the intrinsic parity of O is positive. Although its intrinsic parity is positive, it couples to negative parity states as well.¹⁷

We consider the asymptotic behavior of the correlator in the 5Q CM frame as

$$G_{\alpha\beta}(t) \equiv \frac{1}{V} \sum_{\vec{x}} \langle O_{\alpha}(t, \vec{x}) \bar{O}_{\beta}(0, \vec{0}) \rangle, \quad (3)$$

where V denotes the spatial volume. In the region of $0 \ll t \ll N_t$ (N_t : temporal lattice size), the correlator is decomposed into two parts as

$$G(t) \equiv P_+ \left(C_+ e^{-m_+ t} - C_- e^{-m_-(N_t - t)} \right) \\ + P_- \left(C_- e^{-m_- t} - C_+ e^{-m_+(N_t - t)} \right), \quad (4)$$

where m_{\pm} refer to the energies of lowest-lying states in positive and negative parity channels, respectively. $P_{\pm} \equiv (1 \pm \gamma_4)/2$ serve as projection matrices onto the ‘‘upper’’ and ‘‘lower’’ Dirac subspaces, respectively, in the standard Dirac representation. Eq. (4) suggests that, in the region of $0 \ll t \ll N_t/2$, the backwardly propagating states can be neglected. Hence, ‘‘upper’’ Dirac subspace is dominated by the lowest-lying positive parity state, whereas ‘‘lower’’ Dirac subspace is dominated by the lowest-lying negative parity state. We utilize this property in parity projection.

3. Numerical Result with standard BC

In Fig. 1, we show the effective mass plots for both the parity channels adopting Eq. (1). The effective mass is defined as

$$m_{\text{eff}}(t) \equiv \log(g(t)/g(t+1)), \quad (5)$$

where $g(t)$ denotes correlator in Dirac ‘‘upper’’ or ‘‘lower’’ subspaces. Formally, $g(t)$ can be expressed as a sum of exponentials. In the asymptotic region $0 \ll t \ll N_t/2$ in Euclidean time, contaminations of excited states are expected to be reduced. If $g(t)$ is dominated by single exponential corresponding to the lowest-lying mass m , then the effective mass behaves as constant in this region, i.e., $m_{\text{eff}}(t) \sim m$. Owing to this property, the effective mass plot is often used to determine the fit range.¹⁷

For both the parity channels, we find plateaus in the region $25 \leq t \leq 35$, where single-exponential dominance is expected to be achieved. We simply neglect the data for $t > 35$, where contributions from the backward propagations are seen to become less negligible. The single-exponential fit is performed in the plateau region. The results are denoted by solid lines. The dotted lines indicate the p-wave (s-wave) NK thresholds for positive (negative) parity channels on the spatial lattice size $L \simeq 2.15$ fm. Note that due to the quantized spatial momentum in the finite box, the p-wave threshold is raised as $E_{\text{th}} \simeq \sqrt{m_N^2 + \vec{p}_{\text{min}}^2} + \sqrt{m_K^2 + \vec{p}_{\text{min}}^2}$ with $|\vec{p}_{\text{min}}| = 2\pi/L$.

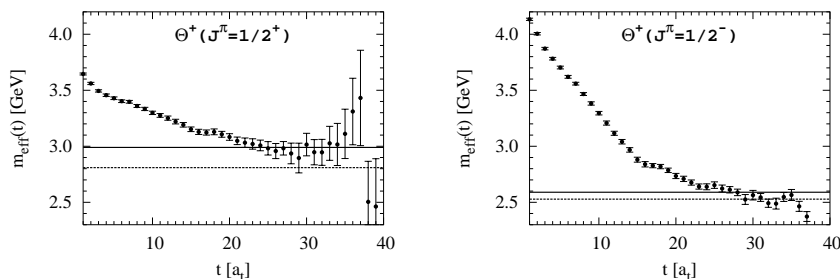


Figure 1. The effective mass plots of positive and negative parity Θ^+ adopting Eq. (1). The solid lines denote the result of the single-exponential fit performed in the region, $25 \leq t \leq 35$. The dotted lines denote the p-wave (s-wave) NK threshold energy for positive (negative) parity channels on the spatial lattice size $L \simeq 2.15$ fm.

In Fig. 2, the masses of positive (triangle) and negative (circle) parity Θ^+ are plotted against m_π^2 . The open symbols denote direct lattice data. We find that the data behaves linearly in m_π^2 . Such a linear behavior against m_π^2 is also observed for ordinary non-PS mesons and baryons.^{13,14} We extrapolate the lattice data linearly to the physical quark mass region. The results are denoted by closed symbols. For convenience, we show p-wave (upper) and s-wave (lower) NK threshold with dotted lines.

In the positive parity channel, the chiral extrapolation leads to $m_\Theta = 2.25$ GeV. Since it is too massive, it cannot be identified with the experimentally observed $\Theta^+(1540)$. In contrast, in the negative parity channel, the chiral extrapolation leads to $m_\Theta = 1.75$ GeV, which is rather close to the empirical value. In order for this to be identified with $\Theta^+(1540)$, it should be confirmed that the observed state is not a NK scattering state but a compact 5Q resonance state. We will pursue this direction in the next section.

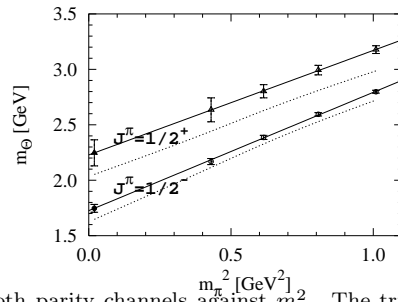


Figure 2. m_Θ for both parity channels against m_π^2 . The triangles correspond to the positive parity, while the circles correspond to the negative parity. The open symbols denote direct lattice data, whereas the closed ones the results after the chiral extrapolation. The dotted lines indicate the NK threshold energies for p-wave (upper) and s-wave (lower) cases.

4. Further investigation with hybrid BC

In the positive parity channel, NK scattering states are in p-wave. Hence, in the 5Q CM frame, the minimum momenta of N and K are non-zero, i.e., $|\vec{p}_{\min}| = 2\pi/L$ (L : the spatial size of the lattice), through which the NK threshold energy acquires the explicit volume dependence as $E_{\text{th}} \simeq \sqrt{m_N^2 + \vec{p}_{\min}^2} + \sqrt{m_K^2 + \vec{p}_{\min}^2}$. This can be utilized to determine whether the state of concern is a compact resonance or a NK scattering state. On the other hand, in the negative parity channel, NK scattering states are in s-wave. Hence, in the 5Q CM frame, N and K can have zero spatial momentum, and the NK threshold energy does not have an explicit volume dependence, i.e., $E_{\text{th}} \simeq m_N + m_K$. This is not convenient for our purpose.

We may ask ourselves whether there could be some prescription which can provide s-wave NK threshold energy with an explicit volume dependence as the p-wave one. This is achieved by twisting the spatial boundary

Table 1. The *hybrid boundary condition (HBC)* imposed on the quark fields. The second line shows the standard (periodic) BC for comparison.

	u quark	d quark	s quark
HBC	anti-periodic	anti-periodic	periodic
standard BC	periodic	periodic	periodic

condition (BC) of quark fields in a flavor dependent manner as follows. We impose the anti-periodic BC on u and d quark fields, while periodic BC on s quark field. We will refer to this boundary condition as “*hybrid boundary condition (HBC)*”. (See Table 1.)

Under HBC, hadrons are subject to their own spatial BC. For instance,

since $N(uud, udd)$ and $K(u\bar{s}, d\bar{s})$ contain odd numbers of u and d quarks, they are subject to the anti-periodic BC. In contrast, since $\Theta^+(uudd\bar{s})$ contains even numbers of u and d quarks, it is subject to the periodic BC. (See Table 2.) Recall that, in the box of the size L , the spatial momenta

Table 2. The consequence of the HBC on hadrons

	quark content	spatial BC	minimum momentum	
N	uud, udd	anti-periodic	$(\pm\pi/L, \pm\pi/L, \pm\pi/L)$	$ \vec{p}_{\min} = \sqrt{3}\pi/L$
K	$u\bar{s}, d\bar{s}$	anti-periodic	$(\pm\pi/L, \pm\pi/L, \pm\pi/L)$	$ \vec{p}_{\min} = \sqrt{3}\pi/L$
Θ^+	$uudd\bar{s}$	periodic	$(0, 0, 0)$	$ \vec{p}_{\min} = 0$

are quantized as $p_i = 2n_i\pi/L$ for periodic BC and $(2n_i + 1)\pi/L$ for anti-periodic BC with $n_i \in \mathbf{Z}$. Therefore, Θ^+ can have zero spatial momentum as $|\vec{p}_{\min}| = 0$. In contrast, N and K have non-zero minimum spatial momenta as $|\vec{p}_{\min}| = \sqrt{3}\pi/L$. Thus, under HBC, s-wave NK threshold energy is raised as

$$E_{\text{th}} \simeq \sqrt{m_N^2 + \vec{p}_{\min}^2} + \sqrt{m_K^2 + \vec{p}_{\min}^2}, \quad |\vec{p}_{\min}| = \sqrt{3}\pi/L, \quad (6)$$

whereas a compact 5Q resonance state is expected to be unaffected.

In order to see that HBC does not affect the spatially localized resonance states, we show an example of an established resonance $\Sigma(uds)$ baryon. We select Σ , because it is subject to the periodic BC unlike N. In Fig. 3, we show

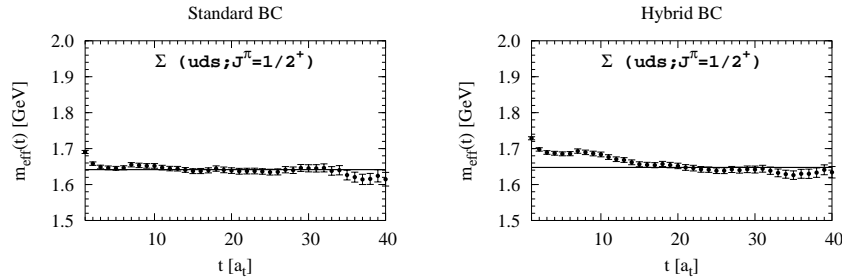


Figure 3. The effective mass plots of $\Sigma(uds)$ under the standard BC and HBC adopting Eq. (1). Solid lines denote the best-fit results performed in the region $20 \leq t \leq 30$.

the effective mass plots of Σ for the standard BC and HBC. The solid lines denote the best-fit results performed in the plateau region as $20 \leq t \leq 30$. There is no significant difference between the two best-fit masses, which shows that HBC does not affect the localized resonance states.

Now we present the HBC result of the 5Q effective mass in the negative parity channel in Fig. 4. The dotted line denotes the modified NK threshold

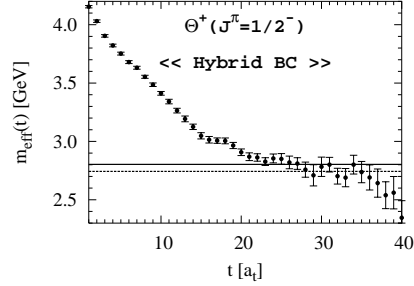


Figure 4. The effective mass plot for the negative parity Θ^+ under HBC adopting Eq. (1). The solid line denotes the result of the best-fit performed in the plateau region as $25 \leq t \leq 35$. The dotted line denotes the s-wave NK threshold Eq. (6). This figure should be compared with the r.h.s. in Fig. 1.

energy due to HBC. Note that the shift of the NK threshold amounts to about 200 MeV in this case, i.e., $L \simeq 2.15$ fm with Eq. (1). We observe that the plateau is raised by consistent amount as the shift of the threshold, which shows that there is no compact 5Q resonance in the region as

$$m_N + m_K \leq E \leq \sqrt{m_N^2 + \vec{p}_{\min}^2} + \sqrt{m_K^2 + \vec{p}_{\min}^2}, \quad |\vec{p}_{\min}| = \sqrt{3}\pi/L. \quad (7)$$

In particular, the plateau observed in the negative parity channel in the previous section turns out to be an NK scattering state.

In Fig. 5, we show the comparison of the results of standard BC (l.h.s.) and HBC (r.h.s.) for each κ . Dots denote the best-fit mass obtained in their plateau region. the solid lines denote the NK threshold energies. We see that, for all κ , the plateaus are raised in a consistent amount as the shift of the NK threshold energies.

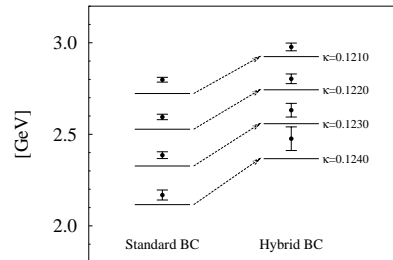


Figure 5. Comparison of the results of standard BC (l.h.s) and HBC (r.h.s.) for each κ . Dots denote the best-fit mass obtained in their plateau regions. The solid lines denote the corresponding NK threshold energies.

5. Summary and Discussion

We have studied the penta-quark Θ^+ state with the quenched anisotropic lattice QCD to provide high-precision data. After the chiral extrapolation, we have obtained $m_\Theta = 2.25$ GeV in the positive parity channel. Since it is too massive, we have concluded that it cannot be identified with the experimentally observed $\Theta^+(1540)$. In contrast, in the negative parity channel, we have obtained $m_\Theta = 1.75$ GeV, which is rather close to the empirical value. In order to confirm that this state is a compact 5Q resonance, we have proposed a new general method with “*hybrid boundary condition (HBC)*”. The HBC analysis has showed that the observed states in the negative parity channel are NK scattering states for all values of κ .

We have thus observed no relevant signals on the compact 5Q resonance in both the parity channels. To reveal the mysterious nature of $\Theta^+(1540)$, more systematic investigations seem to be necessary. In the future study, it is desirable to examine the large volume effect, the dynamical quark effect, different interpolating fields including highly non-local ones, and different quantum numbers other than $J = 1/2, I = 0$.

References

1. LEPS Collaboration, T. Nakano *et al.*, *Phys. Rev. Lett.* **91**, 012002 (2003).
2. D. Diakonov, V. Petrov and M.V. Polyakov, *Z. Phys.* **A359**, 305 (1997).
3. For a review, M. Oka, *Prog. Theor. Phys.* **111**, 1 (2004) and its references.
4. S.L. Zhu, *Int. J. Mod. Phys.* **A19**, 3439 (2004) and its references.
5. T. Nakano and K. Hicks, *Mod. Phys. Lett.* **A19**, 645 (2004).
6. A.W. Thomas, K. Hicks and A. Hosaka, *Prog. Theor. Phys.* **111**, 291 (2004).
7. F. Csikor, Z. Fodor, S.D. Katz and T.G. Kovacs, *JHEP* **0311**, 070 (2003).
8. S. Sasaki, *Phys. Rev. Lett.* **93**, 152001 (2001).
9. T.W. Chiu and T.H. Hsieh, hep-ph/0403020.
10. N.Mathur, F.X.Lee, A.Alexandru, C.Bennhold, Y.Chen, S.J.Dong, T.Draper, I.Horváth, K.F.Liu, S.Tamhankar and J.B.Zang, hep-ph/0406196.
11. H. Suganuma, T.T. Takahashi, F. Okiharu and H. Ichie, *Proc. of QCD Down Under*, Adelaide, March 2004, *Nucl. Phys.* **B** (Proc. Suppl.) in press; F. Okiharu, H. Suganuma and T.T. Takahashi, hep-lat/0407001.
12. T.R. Klassen, *Nucl. Phys.* **B533**, 557 (1998).
13. H. Matsufuru, T. Onogi and T. Umeda, *Phys. Rev.* **D64**, 114503 (2001).
14. Y. Nemoto, N. Nakajima, H. Matsufuru and H. Suganuma, *Phys. Rev.* **D68**, 094505 (2003).
15. N. Ishii, H. Suganuma and H. Matsufuru, *Phys. Rev.* **D66**, 094506 (2002); *Phys. Rev.* **D66**, 014507 (2002).
16. N. Ishii, T. Doi, H. Iida, M. Oka, F. Okiharu, H. Suganuma, hep-lat/0408030.
17. I. Montvay and G. Münster, “*Quantum Fields on a Lattice*”, (Cambridge Univ. Press, Cambridge, England, 1994), p. 1.